03,05,12

Absorption of microwave radiation and magnetoresistance oscillations in InAs/GaSb composite quantum wells with inverted band spectrum in a quantizing magnetic field (Review)

© M.P. Mikhailova, E.V. Ivanov¶, P.V. Semenikhin, R.V. Parfeniev

Ioffe Institute,
St. Petersburg, Russia
¶ E-mail: Ed@mail.ioffe.ru

Received October 24, 2023
Revised December 22, 2023
Accepted February 11, 2024

Magnetotransport properties of the nanoheterostructures based on InAs/GaSb composite quantum wells with a semimetal band spectrum grown by metal organic vapor phase epitaxy on n-GaSb and n-InAs substrates with different carrier concentrations are discussed. The experimental results were obtained by means of the contactless technique of electron paramagnetic resonance at the study of temperature and angular dependences of microwave radiation absorption and magnetoresistance oscillations in the wide range of temperature (2.7−270 K) and magnetic field (up to 1.4 T). The possibility of using electron paramagnetic resonance spectroscopy to study spin-dependent phenomena in two-dimensional heterostructures with an inverted band spectrum in magnetic field has been demonstrated. In particular, we discuss the magnetophonon oscillations of magnetoresistance caused by resonant scattering of $2D$-electrons on interface acoustic phonons in the quantizing magnetic field, which were discovered and investigated in heterostructures with InAs/GaSb quantum wells grown on n^0-InAs substrate.

Keywords: InAs/GaSb composite quantum well, inverted band spectrum, electron paramagnetic resonance, absorption of microwave radiation, acoustic phonons, Shubnikov-de Haase oscillations, magnetophonon oscillations of magnetoresistance.

DOI: 10.61011/PSS.2024.03.57931.240

1. Introduction

The heterostructures based on the InAs/GaSb quantum wells attract attention of the scientific community in relation to studying their properties changing due to transformation of the band structure in the electric and magnetic field, observing band hybridization as well as studying a transition from a semi-metal state of the system (an inverted band order) to a topological isolator [1–6]. The appearance of gybridization gap was investigated in the studies [7–10]. Prospects of the heterostructures with the InAs/GaSb composite quantum wells (CQW) for such studies and creation of new nanoelectronics and spintronics instruments were first mentioned in the theoretical study [11]. Experimental results of investigation of the quantum spin Hall effect with the Fermi level within the hybridization gap of the electron-hole states [1,2,12], as well as an edge transport [2], magnetotransport and spin-dependent phenomena are described in the studies [9,11,13–16]. The study [17] mentions the possibility of creating hybrid structures with superconducting layers.

The InAs, GaSb, AlSb compounds belong to a semiconductor family with similar values of the crystal lattice parameter (6.1 Å) [13], thereby making it possible to grow isoperiodic structures based thereon. A unique property of the InAs/GaSb system is that the InAs conduction band is located below the GaSb valence band by the value of $\Delta = 150$ meV [11,13], while the electron and hole subbands are located in the different CQW layers. As a result, we can observe mixing of the InAs conduction band states with the GaSb valence band states and hybridization of these states under the effect of the electric [9,11,13–15] and magnetic [1,2,9,12,14–16,18] fields. The InAs-GaSb system has another important advantage in a low value of the effective mass of electrons in InAs and a high value of the g-factor in GaSb. The transport and topological properties as well as the Hall effect have been studied in these systems at low temperatures on the structures grown by molecular-beam epitaxy (MBE) [1,2].

In the present study, the AlSb/InAs/GaSb/AlSb CQWs have been grown for the first time using the method of metal-organic vapor phase epitaxy (MOVPE) on three types of the isoperiodic substrates: n-GaSb, n-InAs and n^0-InAs. The technique of obtaining the InAs/GaSb composite quantum wells with a type II broken-gap heterojunction by the MOVPE method has been developed in an Infrared optoelectronics laboratory of Ioffe Institute of the Russian Academy of Sciences together with Institute of Physics of Czech Academy of Sciences [19]. Previously, this technique was successfully applied when growing the deep

Al(As)Sb/$InAs_{1-x}Sb_x$/Al(As)Sb quantum wells, which for the first time exhibited intense superlinear electroluminescence and increase in optical power due to an effect of impact ionization within the temperature range 77−300 K [20]. The studies [21–24] have represented a large cycle of investigation of vertical transport and the resonance low-temperature tunneling processes in the heterostructures with the two-barrier InAs/GaSb/AlSb composite quantum wells in the strong magnetic fields. However, the magnetotransport properties of this type of the structures have not been previously studied by the electron paramagnetic resonance (EPR) method at absorption of microwave radiation.

Using the EPR method we have studied the magnetotransport properties of the AlSb/InAs/GaSb/AlSb CQW-based structures with an inverted band spectrum, which were grown on the various types of the substrates. We have shown applicability of the EPR spectroscopy as a tool for investigating the two-dimensional structure in order to study new spin-dependent physical phenomena that are related to variability of the band structure under the effect of the microwave radiation and the magnetic fields. The EPR technique used by us does not require formation of electric contacts and can record magnetoresistance within the wide temperature range (2.7−300 K) in the quantizing magnetic fields up to 1.4 T. As a result, we have obtained and studied field dependences of the frequency and amplitude of the oscillations as well as temperature and angular dependences of absorption of the microwave radiation in the magnetic field.

2. Technique for measurements based on the spectroscopy of electron paramagnetic resonance

The EPR effect is resonance absorption of electromagnetic radiation by paramagnetic centers in the constant magnetic field. This phenomenon is caused by transitions between energy sublevels of unpaired electrons at Zeeman level splitting.

The EPR-spectroscopy method is widely applied for studying the free and bonded electrons in the two-dimensional and bulk ($3D$) semiconductors, the paramagnetic centers in dilute semiconductors, and for investigating the electron structure of the atoms, magnetic ordering and superconductivity [25–27]. Absorption of the microwave radiation in moderate magnetic fields also enables obtaining information about impurities of interacting and non-interacting ions [28,29]. This peculiarity of the EPR technique means that it is possible to study both the electron shells of the impurity atoms and the kinetics of the electron gas in bulk and low-dimensional materials [30]. A separate experimental field is based on using the EPR spectroscopy for investigating the spin-orbit interaction and the mechanisms of spin relaxation [25].

The microwave radiation can be absorbed in the magnetic field not only as result of interaction with the unpaired electrons, but due to change of the sample resistance as well (the magnetoresistance effect, the Shubnikov-de Haase effect). For this reason, the EPR method has proven to be a multi-function and sensitive tool for studying the magnetoresistance effects [30,31]. At the same time, a task of measuring the spin concentration is solved by comparing a studied and a reference sample.

In the EPR spectrometer the studied sample in a thin-wall cryostat is placed in antinode of the microwave magnetic field of the cavity resonator. Owing to this arrangement, the conducting sample does not distort the microwave field and the resonator keeps a high Q factor. The electromagnetic radiation of the microwave range is generated by a klystron to be passed via a waveguide to the sample, where it is partially absorbed, while unabsorbed radiation is recorded by a detector. The magnetic field is swept at the constant frequency of the microwave radiation. Power of radiation reflected by the resonant cavity is determined by a ratio of impedances of the waveguide and the resonant cavity. In a classic scheme of the EPR measurements, power drop due to sample absorption has a resonance maximum, wherein there is a spin-flip transition between the energy levels under the effect of the electromagnetic wave. As a result, the spin transition takes away standing-wave energy of the magnetic component in the resonant cavity to pass it to the lattice. The modern EPR systems have the detector signal modulated by the weak high-frequency magnetic field. Owing to it, we can record not microwave radiation power absorbed in the sample P, but rather its magnetic field derivative dP/dH, thereby improving sensitivity of the technique and separating magnetic absorption from a part that does not depend on the magnetic field.

As said above, along with EPR, the semiconductors and the heterostructures exhibit non-resonance change of microwave absorption in the magnetic field [31–34], wherein a non-contact technique of the EPR spectrometry makes it possible to study both the types of the said effects [31]. The main phenomenon responsible for change of microwave absorption in the semiconductor is a classic magnetoresistance effect, wherein resistivity of a non-degenerate semiconductor increases in proportion to a square of the applied magnetic field. The power losses during the magnetotransport measurements are caused by spending the energy of the electromagnetic wave to acceleration of the conductivity electrons. The dependence of the absorbed power of microwave radiation on the strength of the magnetic field has a resonance nature. This peculiarity underlies investigation of the magnetoresistance effect using the EPR method.

In most cases, the transport parameters of the system can be determined from the Hall measurements and the Shubnikov-de Haase (SdH) oscillations in the samples with the contacts at direct current conditions. If there is no such possibility, the measurements can be carried out using a non-contact technique of microwave detection of the SdH oscillations in the EPR setup. In doing so, the magnetotransport parameters measured using the EPR

technique well agree with the data obtained by applying other methods [30,31,35]. At the same time, experimental use of the microwave field results in some peculiarities in comparison with the direct current measurements. One of them is related to existence of a skin effect that results in penetration of the microwave field only into the sub-surface area of the studied sample to a skin-layer depth, and in determination of magnetic conductivity by resistance of this area. The skin-layer thickness of our samples is several micrometers. Another peculiarity in using the EPR spectroscopy for such measurements is that accuracy of measurement for absolute values of magnetoresistance is not high ($\sim 20\%$) [36].

The study of magnetotransport properties of the semiconductors and the semimetals by the EPR method based on investigation of the SdH effect. This effect consists in oscillating behavior of conductivity depending on the magnetic field when crossing the Fermi with the Landau levels provided that the conditions of quantization of current carriers are met [37]. With the constant value of the frequency of the microwave radiation, the magnetic field is swept, thereby resulting in the oscillating behavior of magnetoresistance (conductivity), which can be recorded as change in absorption of the microwave radiation. The alternating electromagnetic radiation of the microwave range generates dissipative currents in the sub-surface layer of the sample. At the same time, the constant magnetic field enables distinguishing contribution of the two-dimensional carriers to the conductivity through the spectra of the SdH oscillations, as the signal of the EPR detector is directly proportional to the first derivative of resistance with respect to the magnetic field.

In case of the two-dimensional heterostructures, the angular dependences of the spectra of the SdH oscillations in the magnetic field can be analyzed to separate contributions of the charge carriers in the quantum well and in the substrate, while studying the temperature dependences of absorption of the microwave radiation can help determine the corresponding values of the concentration of the charge carriers [38,39].

In our experiments, we have used the EPR spectrometer E-112 (produced by „VARIAN") with a continuous-flow helium cryostat „Oxford Instruments ESR-910" that maintained the sample temperature with a high accuracy within a wide range of the values ($2-270$ K). The constant magnet solenoids provided sweeping of the magnetic field with the strength up to 14 kOe (1.4 T). The microwave radiation was sourced by the klystron that is designed to operate at the frequency of 9.35 GHz, which corresponds to the quantum energy of $\hbar\omega \approx 0.04$ meV. The power of generated radiation was ~ 1 mW. The experiments were made on the setup designed to study the change of magnetoresistance in the two-dimensional structures [30] in addition to the classic technique for investigating the spin ordering and interaction of the paramagnetic centers in the bulk samples [31,34]. In order to obtain the angular dependences of magnetoresistance that correspond to a different orientation of the vector $\boldsymbol{H}$ in relation to the epitaxial layers of the heterostructure, the studied samples were rotated in the magnetic field as shown in Figure 1.

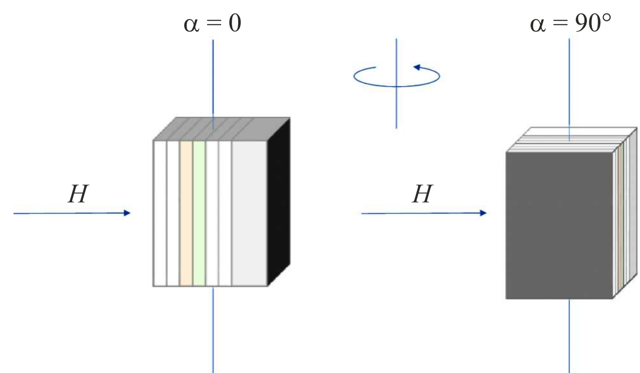

Figure 1. Diagram for recording the angular dependences of absorption of the microwave radiation and the oscillations of magnetoresistance of the two-dimensional heterostructures by the EPR spectroscopy method (α — the angle between the vector $\boldsymbol{H}$ and the structure growth direction).

3. Technique of heterostructure manufacturing

The AlSb/InAs/GaSb/AlSb CQWs were grown by the MOVPE method in the AIXTRON 200 machine in a horizontal quartz reactor with a non-rotating RF heated graphite holder [19]. The machine included a temperature monitoring system and a system Laytec EPIRAS 200TT designed to control the growth process *in situ* by the anisotropic reflection spectroscopy method (RAS) [40–43].

As the precursors for the grown compounds triethylgallium TEGa, tri(tertiarybutyl)aluminum TtBAl, trimethylindium TMIn, triethylstibine TESb or trimethylstibine TMSb and tertiarybutylarsine TBAs were used. The heterostructures were grown in the hydrogen atmosphere at the temperature of 560°C and under the pressure of 150 hPa. Before the epitaxial growth, the oxide film was removed from the substrate surface by means of the HCl water solution to be subsequently flushed by water and isopropyl alcohol. The substrates prepared for epitaxy were loaded into the reactor and subjected to thermal deoxidation at the temperature of 560°C.

The structures for study (QW2505A, QW2505B and QW2550C, as shown in Figure 2) were grown on the three types of the substrates with low concentrations of the charge carriers: n-GaSb: Te (100) ($n = 3 \cdot 10^{17}\,\text{cm}^{-3}$), n-InAs: Mn (100) ($n = 1.1 \cdot 10^{17}\,\text{cm}^{-3}$) and undoped n-InAs (100) ($n \approx 10^{16}\,\text{cm}^{-3}$), respectively. The n-InAs substrate was doped by a Mn impurity in order to change the electron concentration. The magnetic nature of the impurity did not affect the results that we obtained in the experiments by means of the EPR non-contact technique.

After etching and deoxidation, a buffer layer was deposited on the substrate to smooth surface irregularities before growing the active area. The GaSb buffer layer of the thickness of 100 nm was grown in the QW2505A and QW2505B heterostructures. In case of the QW2550C heterostructure, the buffer was a 30 nm InAs layer. The InAs/GaSb CQW included two single quantum wells, such as InAs of the width of $d = 12.5$ nm and GaSb of $d = 8$ nm and on both sides it was restricted by the AlSb barriers (30 nm each). The quantum wells, the barrier and buffer layers were intentionally undoped. The thin covering GaSb layer (3–6 nm) was used to protect the upper AlSb barrier against oxidation. The parameters of the AlSb/InAs/GaSb/AlSb CQWs (the materials, the thickness values of the layers and the barriers as well as their sequence) were the same for all the structures.

Perfection of the grown heterostructures was checked using transmission electron microscopy (TEM). Based on the obtained results, structures were selected for further experiments. Dispersion of the width of the AlSb/InAs/GaSb quantum wells in the nanoheterostructures that were studied later by the EPR method can be evaluated as a value of about several angstroms. The measurement samples were shaped as parallelepipeds with the sizes $6 \times 3 \times 0.35$ mm.

At the InAs/GaSb heterointerface, both the atoms groups III and V are interchangeable. Then, the interface can be grown both as InSb-like and as AlAs-like. The interface type substantially affects the band structure of the quantum wells, since the band gap widths of the said materials are quite different (at $T = 300$ K $E_g = 0.18$ and 2.16 eV for InSb and AlAs, respectively). As shown in the study [44], in the semiconductor heterostructures III–V, the band overlapping substantially depends on the type and quality of the interface monolayer. In our case, the InSb-like interface is the only possible option in terms of creating the InAs/GaSb CQW with the inverted band spectrum. Besides, this interface provides for higher values of mobility of the charge carriers [45,46]. It should be noted that the heterointerfaces also can have the InSb-like or AlSb-like interfaces formed between the AlSb barriers and the InAs/GaSb CQWs. In accordance with the experimental results, realization of the InSb-like interfaces at the said heteroboundaries turned out to be more preferable, since it can reduce the strains in the heterostructure [19]. The interfaces with a higher Sb content were obtained by using a special sequence of deposition of the metal-organic compounds during growing [47].

The thicknesses in the InAs/GaSb layers were selected on a condition of obtaining the semimetal (inverted) band structure [13]. Previously, the studies [1,11,18,48] have calculated the energy band diagrams of the respective heterostructures. It is shown that in the InAs narrow well of the width of $d < 8.5$ nm the ground level of the quantum states of the electrons E_{e1} is above the ground level of the heavy holes E_{h1} in GaSb, which corresponds to the classic semiconductor structure. In case of the wider InAs quantum wells, the structures gets the inverted order of the energy bands, i. e. the magnitude $(E_{e1} - E_{h1})$ becomes negative. It is assumed that the carriers are spatially separated, but due to Coulomb interaction the electrons flow from the InAs valence band, forming a band bend at the heterojunction (see below in Figure 5).

QW2505A	QW2505B	QW2550C
GaSb – 3 nm	GaSb – 3 nm	GaSb – 6 nm
AlSb – 30 nm	AlSb – 30 nm	AlSb – 30 nm
GaSb – 8 nm	GaSb – 8 nm	GaSb – 8 nm
InAs – 12.5 nm	InAs – 12.5 nm	InAs – 12.5 nm
AlSb – 30 nm	AlSb – 30 nm	AlSb – 30 nm
GaSb – 100 nm	GaSb – 100 nm	InAs – 30 nm
n-GaSb : Te ($n = 3 \cdot 10^{17}$ cm^{-3})	n-InAs : Mn ($n = 1.1 \cdot 10^{17}$ cm^{-3})	n-InAs ($n = 10^{16}$ cm^{-3})

Figure 2. Schematic diagrams of the heterostructures with the InAs/GaSb composite quantum wells with the semimetal band spectrum, which are grown by metalorganic vapour phase epitaxy on the substrates GaSb and InAs.

4. Experimental results

4.1. AlSb/InAs/GaSb/AlSb structure on the n-GaSb substrate

For the QW2505A heterostructure (Figure 2) with the InAs/GaSb CQW grown on the n-GaSb substrate: Te (100) with the carrier concentration $n = 3 \cdot 10^{17}$ cm^{-3}, it has studied the spectra of absorption of the microwave radiation depending on the direction of the magnetic field using the EPR technique. The spectra have exhibited the clearly distinguished SdH oscillations within the range of the fields from 0.4 T to 1.4 T, which disappear at the temperature above 20 K [49,50]. No spin splitting of the Landau levels was detected in the heterostructure under study. This result requires additional investigation, since in case of the two-dimensional structures the spin effects in the Shubnikov-de Haase oscillations in certain conditions can be manifested even at the moderate magnetic fields in comparison with the bulk materials [51].

The temperature dependence of the amplitude of the SdH oscillations as shown in Figure 3 was analyzed to determine a value of the effective mass of the charge carriers. Using the formula proposed in the study [52], we have obtained the value of the effective mass $m^* = 0.027m_0$, where m_0 — the electron mass. The value of mobility of the 2D-carriers in the InAs quantum well as determined from the respective experimental data was $\mu_e = 70900$ cm^2/V · s.

Rotation of the heterostructure in the magnetic field has revealed an unusual angular dependence of the amplitude of the SdH oscillations that was different from the expected

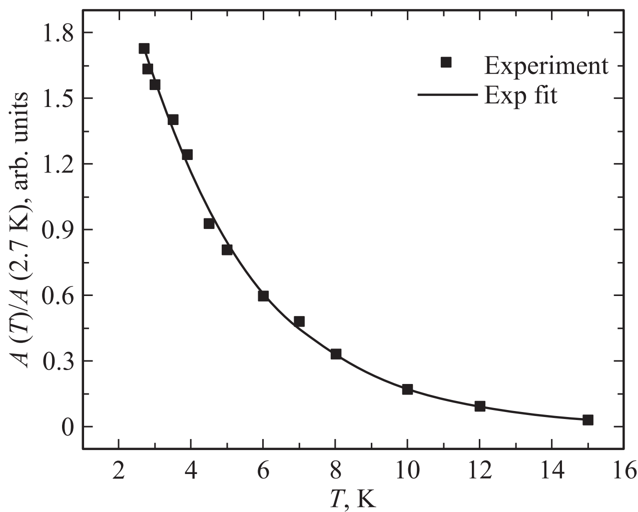

Figure 3. Temperature dependence of the amplitude of the Shubnikov-de Haase oscillations in the magnetic field of 1.4 T for the QW2505A heterostructure with the InAs/GaSb composite quantum well grown on the n-GaSb: Te substrate.

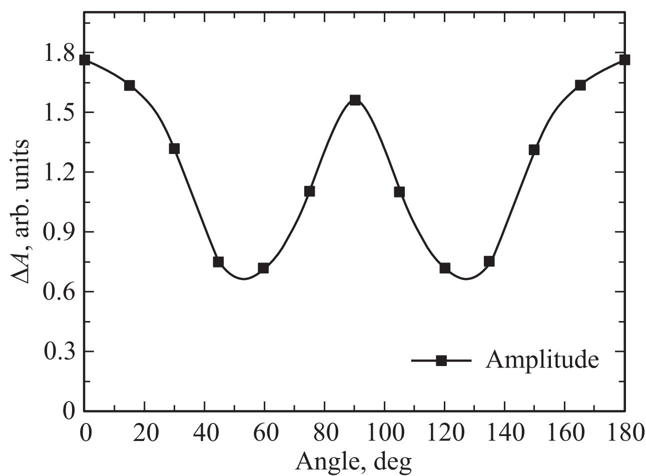

Figure 4. Angular dependence of the amplitude of the Shubnikov-de Haase oscillations for the QW2505A heterostructure in the magnetic field of 1.4 T at the temperature of $T = 2.7$ K.

function $H \cos\alpha$, which is typical for a gas of the two-dimensional carriers [30]. The studied samples was rotated around the axis [001]. Accordingly, the values of the angle $\alpha = 0$ and 90° (see Figure 1) correspond to the orientation when the vector $\boldsymbol{H}$ is parallel to the directions [100] and [010].

The experimentally-recorded angular dependence of Figure 4 is a specific feature of bulk inversion asymmetry (BIA) and caused by absorption of microwave radiation by the charge carriers in the n-GaSb substrate [53,54]. The BIA effect is typically present in the semiconductors III–V with a zinc blende structure without the inversion center [45,46].

The inversion asymmetry in the bulk semiconductors and the heterostructures results in spin splitting of the conduction band [55]. The study [39] has theoretically and experimentally investigated this phenomenon (caused by the BIA effect) in the material n-GaSb: Te. For the samples with the carrier concentration $n > 10^{18}\,\mathrm{cm}^{-3}$ and the Fermi energy $E_F = 0.096$ eV it have been obtained a value of maximum spin splitting on the Fermi surface $(C_2 E_F) = 0.005$ eV, where $C_2 = 0.05$ — the parameter of spin splitting, which was introduced by the authors of the quoted article. In our case, the carrier concentration in the n-GaSb substrate is $n = 3 \cdot 10^{17}\,\mathrm{cm}^{-3}$, and the Fermi energy $E_F = 125$ meV. Thus, using the results of the study [39], the maximum spin splitting of the conduction band in the n-GaSb substrate related to bulk inversion asymmetry can be determined as $\Delta_{\mathrm{BIA}} \sim C_2\, E_F \approx 0.006$ eV.

It should be noted that the Dresselhaus parameter for gallium antimonide is $\gamma_D \approx 187\,\mathrm{eV}\cdot\text{Å}^3$ [56,57]. Hence, by means of the expression

$$k_F = (2m^* E_F)^{1/2}/\hbar, \tag{1}$$

where k_F — the value of the Fermi wave vector, $m^* = 0.041 m_0$ [58], we obtain the following evaluation: $k_F \approx 3.7 \cdot 10^8\,\mathrm{m}^{-1}$, $\Delta_{\mathrm{BIA}} \sim \gamma_D k_F^3 \approx 0.009$ eV. The latter result quite well agrees with the above-found value Δ_{BIA} for the n-GaSb substrate.

Together with the BIA effect, in the semiconductor heterostructures the spin splitting of the conduction band is also caused by structural inversion asymmetry (SIA) [53,55,59]. Generally, the spin splitting is anisotropic and is a result of complex interaction of the components $\Delta_{\mathrm{BIA}} = 2k\beta_D$ and $\Delta_{\mathrm{SIA}} = 2k\alpha_R$, where β_D — the k-linear Dresselhaus parameter, α_R — the Rashba parameter [55,60].

Influence of the BIA and SIA effects on the phenomena of the spin conduction band splitting for the heterostructures with the 50 nm-AlSb/12 nm-InAs/10 nm-GaSb/50 nm-AlSb CQWs was experimentally investigated in the study [61]. The following values of the Rashba and Dresselhaus parameters were obtained, in particular, from analysis of the SdH oscillation: $\alpha_R \approx (0.77-2.0) \cdot 10^{-11}\,\mathrm{eV}\cdot\mathrm{m}$ (depending on the gate voltage V_g, which varied within the range from 0.2 V to −1 V) and $\beta_D \approx 0.2 \cdot 10^{-11}$ eV·m (regardless of the magnitude V_g).

4.2. AlSb/InAs/GaSb/AlSb structure on the n-InAs: Mn substrate

It has also investigated absorption of microwave radiation and the SdH oscillations in the QW2505B structure (see Figure 2) with the InAs/GaSb CQW grown on the n-InAs: Mn (100) substrate with the carrier concentration $n = 1.1 \cdot 10^{17}\,\mathrm{cm}^{-3}$. The measurements were performed within the temperature range 2.7–20 K. The energy band diagram of this structure as shown in Figure 5 was calculated based on a three-band Kane model taking into account band nonparabolicity [24].

For the InAs quantum well of the width of 12.5 nm that contains the electrons with the effective mass

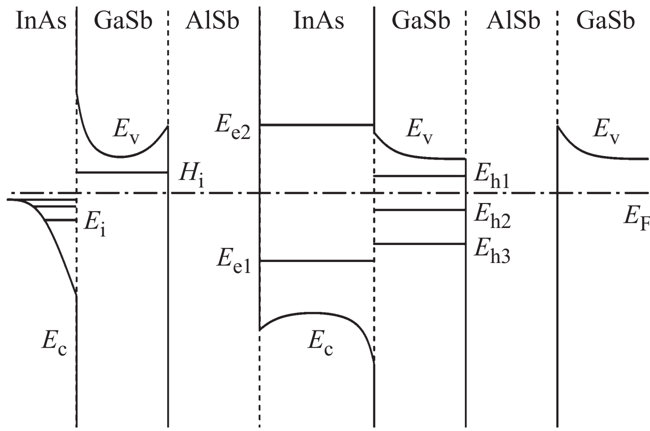

Figure 5. Energy band diagram of the QW2505B heterostructure with the InAs/GaSb composite quantum well grown on the *n*-InAs substrate: Mn ($n = 1.1 \cdot 10^{17}\,\text{cm}^{-3}$).

$m_e = 0.023m_0$, the energy of the two first quantum levels counted from a middle of the InAs band gap takes the values $E_{e1} = 46$ and $E_{e2} = 156\,\text{meV}$. Hence, the second energy level is above the top of GaSb valence band and therefore it is not inside an area of overlapping of the InAs conduction band and the GaSb valence band at the interface (this area has the width of $\Delta = 150\,\text{meV}$).

It should be noted that the value of the parameter Δ can vary depending on the temperature [62]. With increase in the temperature, the band gap of the bulk semiconductor III–V decreases in accordance with the Varshni dependence [58]. A value of deformation potential makes it possible to calculate a shift of the energy levels in relation to the fixed potential value due to the change of the crystal volume. In accordance with these evaluations, with the temperature increasing from 4 to 300 K, an increase in the width of the overlapping area of the InAs conduction band and the GaSb valence band is $\sim 25\,\text{meV}$.

As shown by the subsequent calculation, the GaSb quantum well of the width of 8 nm contains four levels of the heavy holes with the effective mass of $m_{hh} = 0.4m_0$: $E_{h1} = 12\,\text{meV}$, $E_{h2} = 46\,\text{meV}$, $E_{h3} = 103\,\text{meV}$ and $E_{h4} = 181\,\text{meV}$. The last level is beyond the overlapping area of the InAs conduction band and the GaSb valence band. As a result, the effective overlapping of the main electron and hole sub-levels is $\Delta_0 = (\Delta - E_{e1} - E_{h1}) = 92\,\text{meV}$, and the band arrangement is determined by the electrical neutrality relationship $n_{2D} = p_{2D}$, where n_{2D} and p_{2D} — the two-dimensional concentration of electrons and holes in the InAs and GaSb quantum wells, respectively.

The position of the Fermi level E_F in relation to the levels E_{e1} and E_{h1}, and the carrier concentration in the quantum well can be found by means of the expression [63,64]:

$$(E_F - E_{e1})m_e = (\Delta - E_F - E_{h1})m_{hh}. \qquad (2)$$

At the same time, it is assumed that presence of a high potential AlSb barrier makes it possible to neglect a flow of electrons from the substrate into the InAs quantum well. Thus, the semimetal state of the InAs/GaSb CQW is described by position of the Fermi level in relation to the energy levels of the two-dimensional electrons and holes: $E_F - E_{e1} = 86\,\text{meV}$ and $E_{h1} - E_F = 6\,\text{meV}$. Hence, we can find the value of the hole concentration in the GaSb quantum well $p_{2D} = 1.07 \cdot 10^{12}\,\text{cm}^{-2}$.

For the studied heterostructure, the spectra of absorption of microwave radiation from the magnetic field have demonstrated the presence of SdH oscillations at the low temperatures ($T < 10\,\text{K}$) [49]. The angular dependences of the amplitude of these oscillations in the magnetic field (Figure 6) had two sets of the frequencies corresponding to the 2*D*-electrons in the InAs nanolayer and the bulk carriers in the substrate.

Since the Fermi surface in indium arsenide is isotropic, we have proposed a method of analysis of these oscillations to distinguish the contribution of the two-dimensional carriers in the InAs quantum well. First, we have subtracted the oscillations corresponding to the angle $\alpha = 90°$, i. e. the oscillations from the conduction electrons in the *n*-InAs: Mn substrate, from the main set of the experimental results. Then, the obtained dependences were processed by a method of spline interpolation (the Savitsky–Golay method) for the various values of the angles [50].

As can be seen from Figure 6, which shows both the initial and the smoothed curves, with increase in the angle α the spectrum minimum is shifted towards the higher values of the strength of the magnetic field in accordance with the dependence $H\cos\alpha$, which is typical for the 2*D*-carriers.

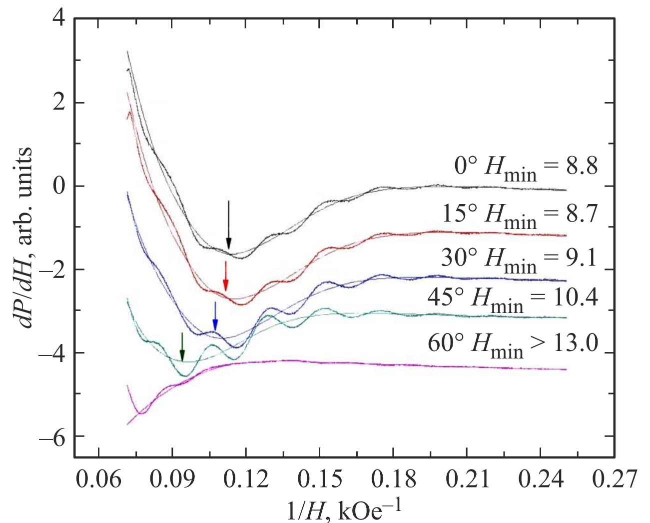

Figure 6. Angular dependences of the amplitude of the Shubnikov-de Haase oscillations on the reverse magnetic field for the QW2505B heterostructure at the temperature of $T = 2.7\,\text{K}$ (the oscillating curves) and the results of their processing by the method of spline interpolation (the curves without the oscillations). For the smoothed dependences, the arrows show the minimum positions, and the respective values of the strength of the magnetic field H_{min} are given in kOe.

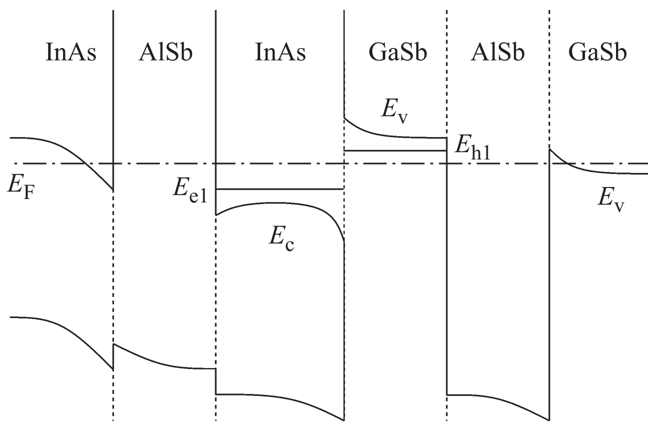

Figure 7. Energy band diagram of the QW2550C heterostructure with the InAs/GaSb composite quantum well grown on the undoped n-InAs substrate ($n \approx 10^{16}\,\mathrm{cm}^{-3}$). The width of the area of overlapping of the InAs conduction band and the GaSb valence band is 150 meV.

The value of the oscillation period was used for calculating the electron concentration in the InAs quantum well. It resulted in obtaining the value $n_{2D} = 3 \cdot 10^{11}\,\mathrm{cm}^{-2}$.

4.3. AlSb/InAs/GaSb/AlSb structure on the undoped n-InAs substrate

Within the wide temperature range from 2.7 to 270 K the method of EPR spectroscopy was used to study the QW2550C heterostructure (Figure 2) with the InAs/GaSb CQW grown on the n-InAs (100) substrate with the carrier concentration near the intrinsic one ($n \approx 10^{16}\,\mathrm{cm}^{-3}$).

The energy band diagram for this structure (Figure 7) shows that the area of overlapping of the InAs conduction band and the GaSb valence band includes one energy level of electrons and three levels of heavy holes: $E_{e1} = 46\,\mathrm{meV}$ and $E_{h1} = 12\,\mathrm{meV}$, $E_{h2} = 46\,\mathrm{meV}$, $E_{h3} = 103\,\mathrm{meV}$. Peculiarity of the heterostructure grown on the undoped InAs substrate is an excessive concentration of holes in the GaSb two-dimensional layer due to their diffusion from the substrate. It results in violation of electrostatic equilibrium between the electrons and the holes in the CQW within the area of overlapping and the concentration of electrons at the level E_{e1} decreases.

Figure 8 shows the spectra of the first derivative of absorption of microwave radiation in the magnetic field dP/dH for the two temperatures depending on orientation of the magnetic field in relation to the direction of growth of the two-dimensional layers of the heterostructure. At $T = 2.7\,\mathrm{K}$ and the value of the angle $\alpha = 90^\circ$ it has exhibited only the SdH oscillations from the $3D$-electrons in the substrate, whose amplitude exponentially decreased with increase in the temperature. The value of the period of the said oscillations could make it possible to determine the concentration of the charge carriers in the substrate $n_{3D} \approx 10^{16}\,\mathrm{cm}^{-3}$. The effective mass of electrons at the Fermi level, which was found from the temperature dependence of the amplitude of the SdH oscillations at $\alpha = 90^\circ$ was $m^* = 0.026 m_0$ [65].

As can be seen from Figure 8, with increase in the temperature the SdH oscillations from the bulk electrons quickly decrease in the amplitude. The angular dependence of absorption of microwave radiation unambiguously indicates the $2D$-nature of the detected peculiarities of the spectra dP/dH and can relate them to the two-dimensional charge carriers in the quantum well. A possibility of considering and separating the contributions of two-dimensional and bulk carriers to the magnetoresistence during the non-contact measurements of the derivative dP/dH is demonstrated by us in the study [50]. However, in this case it is difficult to analyze the SdH oscillations from the two-dimensional carriers in the quantum well at $T = 2.7\,\mathrm{K}$ (thereby obtaining the data on the position of the Fermi level and the effective mass of the carriers) due to heavy overlapping of the two sets of the frequencies of the SdH oscillations from the $2D$- and $3D$-carriers. Computer processing of the results could qualitatively confirm existence of the SdH oscillations from the two-dimensional electrons in the quantum well, whose amplitude drops with the temperature faster than in the case of the oscillations from the bulk carriers in the substrate.

The value of the period of the $2D$-SdH oscillations, which is obtained from analysis of the experimental data, has been used for calculating the two-dimensional concentration of the electrons in the InAs nanolayer $n_{2D} = 4 \cdot 10^{10}\,\mathrm{cm}^{-2}$. It could determine the position of the Fermi level in relation to the main energy levels of the electrons and holes in the CQW: $E_F - E_{e1} = 3.3$ meV, $E_{h1} - E_F = 89\,\mathrm{meV}$. Then, based on these values, we have found the concentration of holes in the GaSb nanolayer $p_{2D} = 1.5 \cdot 10^{13}\,\mathrm{cm}^{-2}$.

At the low temperatures, due to modulation of the density of states at the Fermi level under effect of the magnetic field, the degenerate two-dimensional electron gas exhibits not only the SdH oscillations in magnetoresistance, but also magnetophonon oscillations [66] due to resonance scattering of electrons on the optical [67] and the acoustical phonons [68–70].

The magnetophonon oscillations in the semiconductors are studied for quite a long time [67,71], wherein several types of these oscillations that are different in their nature have been discovered [60]. Of particular interest are the magnetoresistance oscillations due to resonance scattering of the electrons located at the Landau levels on the acoustic phonons, i.e. phonon induced resistance oscillations (PIRO). This effect is most pronounced in the $2D$-structures with high mobility of the charge carriers in the moderate magnetic fields [68,70]. The role of the interface and bulk acoustic phonons in appearance of the magnetoresistance oscillations was previously discussed in the review [66]. In our experiments, within the temperature range 2.7–270 K we have found the magnetoresistance oscillations, which can be explained by resonance scattering of the two-dimensional electrons on the acoustic phonons — PIRO [65].

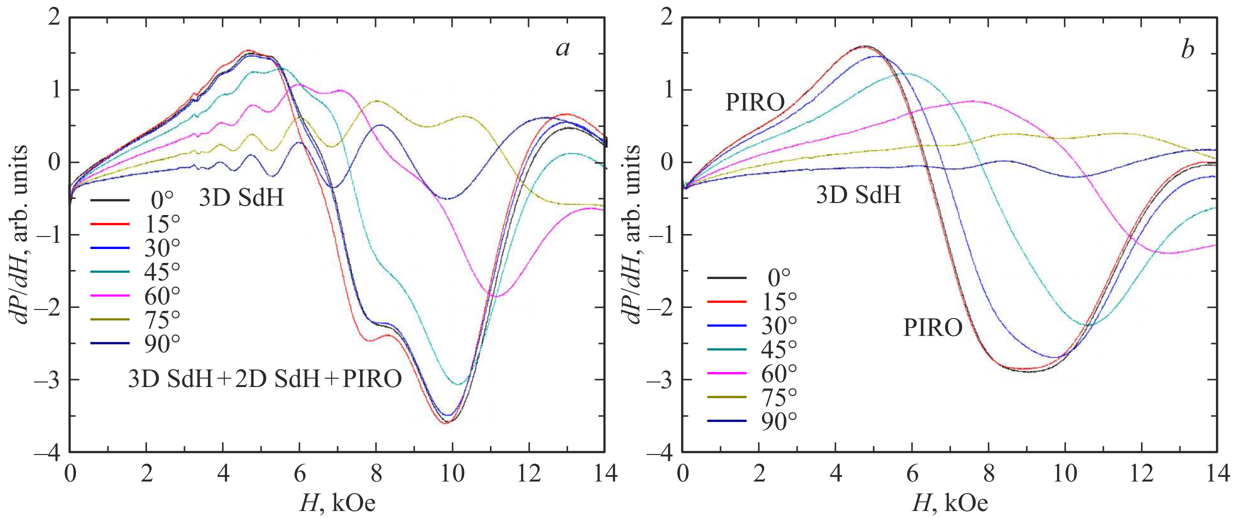

Figure 8. Angular dependences of absorption of microwave radiation in the magnetic field for the QW2550C heterostructure, which are measured at the temperature of 2.7 K (*a*) and 10 K (*b*). The Shubnikov-de Haase oscillations in the substrate (3D SdH), the magnetophonon oscillations (PIRO) and the combined Shubnikov-de Haase oscillations from the bulk and two-dimensional carriers, which are superimposed on the magnetophonon oscillations (3D SdH + 2D SdH + PIRO) are noted.

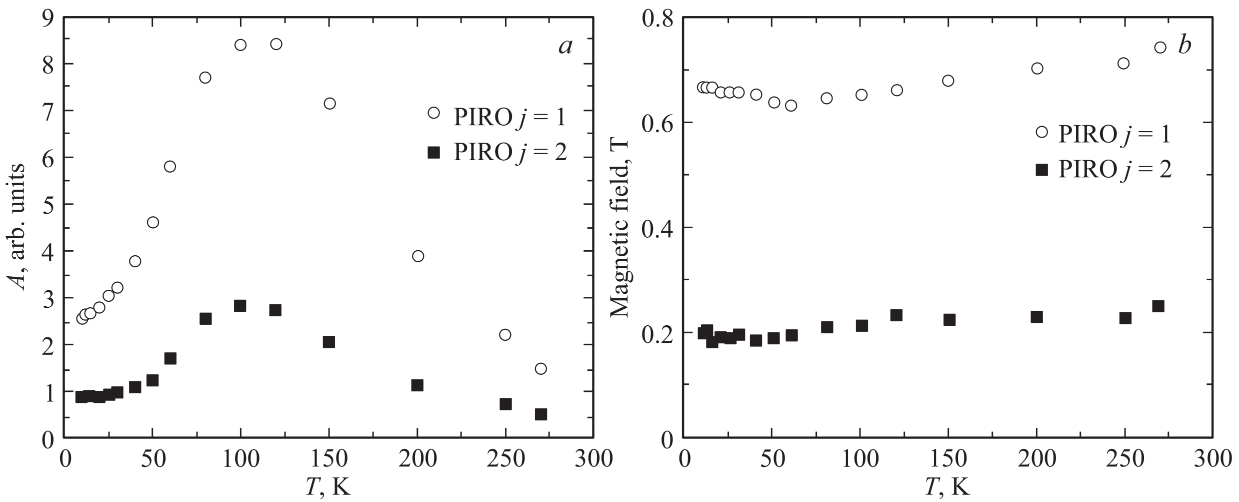

Figure 9. Temperature dependences of the amplitude (*a*) and the position of the maximum (*b*) for the two peaks of the PIRO magnetophonon oscillations $j = 1$ and 2, which are recorded for the QW2550C heterostructure.

The model of interaction of the degenerate two-dimensional electron gas with the phonons having the angular frequency ω_S, the wave vector q and the velocity $v_S = \omega_S/q$ is considered in the study [68–70]. It has been shown that as moving in a quantizing magnetic field, the electron with the Fermi wave vector k_F performs indirect transitions between the Landau levels due to inelastic interaction with the phonon that is characterized by the wave vector $q = 2k_F$. The position of the maximums of the magnetophonon magnetoresistance oscillations of the two-dimensional electron gas is expressed as follows

$$2k_F v_S = j\omega_C, \tag{3}$$

where $\omega_C = eH/(cm^*)$ — the cyclotron frequency, $j = 1, 2, 3, \ldots$ — the integer number.

It should be noted that the bulk phonons are not involved in interaction with the $2D$-electrons, as their frequency depends on a component of the wave vector q_z (where z — the direction of growth of the heterostructure), and the selection rules define only those components of the wave vector that are in the quantum well plane. In our case, the two-dimensional electrons are scattered on the interface phonons propagating along the InAs/GaSb heterointerface.

It is difficult to determine the value of the Fermi wave vector from the spectra of the two-dimensional SdH oscillations due to their complex overlapping with the three-dimensional SdH and with the magnetophonon oscillations as well. However, using the distinguished $2D$-SdH oscillations, we can evaluate the value of k_F by means of the formula (1). From the condition of electrical

neutrality at $n_{2D} \approx 10^{11}\,\mathrm{cm}^{-2}$ we determine a value of $E_F \approx 10\,\mathrm{meV}$, which corresponds to the experimental data for the undoped InAs/GaSb CQWs with the inverted band spectrum [48,72]. Then, using the previously found value of the effective mass $m^* = 0.026m_0$, we obtain $k_F \sim 10^8\,\mathrm{m}^{-1}$.

Figure 9 shows the temperature dependences of the magnetophonon oscillations for the two PIRO peaks. The amplitude of the said oscillations (Figure 9, *a*) has a maximum near the temperature $T_{\max} \approx 120\,\mathrm{K}$. At the same time, for each PIRO peak, a relative amplitude increment observed as the temperature increases within the range $2.7-120\,\mathrm{K}$, is ~ 2.5 times. Further increase in the temperature (at $T > T_{\max}$) results in decrease in the amplitude of the PIRO oscillations in proportion to $T^{-3/2}$. As can be seen from Figure 9, *b*, the position of the resonance peaks of magnetoresistance changes together with the temperature, but the peaks are asymmetrically shifted, thereby indicating the change of the oscillation period after passing over the maximum. This peculiarity is related to the temperature change of mobility of the two-dimensional charge carriers.

The experimental dependences of Figure 9, *a* well agree with the model of thermally activated phonon scattering. At the low temperature, the number of the phonons is small, but they have energy that enables the 2*D*-electrons passing to the higher Landau levels. With increase in the temperature, the number of the thermally activated phonons increases, thereby resulting in increase of the amplitude of the oscillations. As in the case of the SdH oscillations, here it is required the compliance of the value of mobility of the 2*D*-electrons to the condition $(\mu_e H) > 1$, which enables the electron to make several revolutions along the cyclotron orbit.

At the same time, the increase in the temperature is accompanied by spreading of the Landau levels due to the scattering and spreading of the Fermi level of the two-dimensional electrons as well ($2k_F$ spreading). As a result, when achieving the value $T_{\max}$, the subsequent increase in the temperature leads to the drop of the oscillation amplitude. Moreover, due to a difference in the dependences $E_g(T)$ for the materials making up the CQWs [58] the width of the overlapping area of the InAs conduction band and the GaSb valence band is varied with increase in the temperature, thereby resulting, in turn, in the change of the position of the Fermi level. In addition, it should be taken into account that filling of the dimensional quantization levels in CQW depends on the temperature as well. These phenomena explain the temperature shift of the PIRO peaks (Figure 9, *b*), which was observed in our experiments.

5. Conclusion

Thus, the method of electron paramagnetic resonance spectroscopy was used to investigate the magnetotransport properties of the two-dimensional heterostructures based on the InAs/GaSb composite quantum wells with the type II broken-gap heterojunction and the semimetal band structure within the temperature range $2.7-270\,\mathrm{K}$ in the quantizing magnetic field up to 1.4 T.

The studied structures were grown by metal-organic vapor phase epitaxy on three types of the isoperiodic structures with the different carrier concentration: *n*-GaSb: Te ($n = 3 \cdot 10^{17}\,\mathrm{cm}^{-3}$), *n*-InAs: Mn ($n = 1.1 \cdot 10^{17}\,\mathrm{cm}^{-3}$) and n^0-InAs ($n \approx 10^{16}\,\mathrm{cm}^{-3}$). The InAs/GaSb composite quantum wells with the inverted band spectrum were characterized by high mobility of the 2*D*-electrons $\mu_e \approx 7 \cdot 10^4\,\mathrm{cm}^2/\mathrm{V \cdot s}$.

The magnetoresistance oscillations and the Shubnikov-de Haase oscillations were studied by means of the electron paramagnetic resonance non-contact technique. We have studied the field dependences of the frequency and amplitude of the oscillations as well as temperature and angular dependences of absorption of the microwave radiation in the magnetic field.

For the heterostructure with the composite quantum well grown on the *n*-GaSb: Te substrate, we have found the unusual angular dependence of the amplitude of the Shubnikov-de Haase oscillations, which is different from the function $H\cos\alpha$. This effect results from bulk inversion asymmetry (BIA) due to absorption of microwave radiation by the bulk carriers in the *n*-GaSb substrate.

In the AlSb/InAs/GaSb/AlSb heterostructures grown on the *n*-InAs: Mn substrate, in the spectra of absorption of microwave radiation from the magnetic field, we have recorded the Shubnikov-de Haase oscillations, which are characterized by the angular dependence of the amplitude with the two sets of the frequencies corresponding to the 2*D*-electrons in the InAs quantum well and the 3*D*-carriers in the substrate. For the first time we have proposed a method of analyzing these oscillations, which is designed to distinguish the contribution of the two-dimensional carriers to the total conductivity in order to determine their role in the quantum kinetics in the magnetic field.

The two-dimensional structures with the InAs/GaSb composite quantum well, which were grown on the undoped *n*-InAs substrates, have exhibited the magnetophonon oscillations of magnetoresistance of the two-dimensional electron gas in the temperature range $2.7-270\,\mathrm{K}$. It is shown that the said oscillations are caused by resonance scattering of the two-dimensional electrons on the interface acoustic phonons propagating along the InAs/GaSb heterointerface — phonon induced resistance oscillations (PIRO). The amplitude of the magnetophonon oscillations of magnetoresistance reaches the maximum values at the temperature of $\sim 120\,\mathrm{K}$, while the position of the PIRO peaks depends on localization of the Fermi level within the area of overlapping of the InAs and GaSb bands at the interface of the composite quantum well with taking into account filling of the dimensional quantization levels.

The obtained results show that the spectroscopy of electron paramagnetic resonance can be used as an effective tool for studying the properties of the two-dimensional

heterostructures. Thus, it is possible to obtain important information about the resonance and spin-dependent phenomena at absorption of microwave radiation in the quantizing magnetic field within the wide temperature range.

Acknowledgments

The authors would like to thank A.I. Veinger and I.V. Kochman for great contribution to the experimental studies of the two-dimensional heterostructures by the EPR spectroscopy method and for fruitful discussion of the results.

Conflict of interest

The authors declare that they have no conflict of interest.

References

[1] C. Liu, T.L. Hughes, X.-L. Qi, K. Wang, S.-C. Zhang. Phys. Rev. Lett. **100**, *23*, 236601 (2008).
[2] L. Du, I. Knez, G. Sullivan, R.-R. Du. Phys. Rev. Lett. **114**, *9*, 096802 (2015).
[3] X.-L. Qi, S.-C. Zhang. Phys. Today **63**, *1*, 33 (2010).
[4] J.E. Moore. Nature **464**, *7286*, 194 (2010).
[5] J.E. Moore, L. Balents. Phys. Rev. B **75**, *12*, 121306(R) (2007).
[6] M.Z. Hasan, C.L. Kane. Rev. Mod. Phys. **82**, *4*, 3045 (2010).
[7] L.L. Chang, L. Esaki. Surf. Science **98**, *1–3*, 70 (1980).
[8] M. Altarelli. Phys. Rev. B **28**, *2*, 842 (1983).
[9] M.J. Yang, C.H. Yang, B.R. Bennett, B.V. Shanabrook. Phys. Rev. Lett. **78**, *24*, 4613 (1997).
[10] M. Lakrimi, S. Khym, R.J. Nicholas, D.M. Symons, F.M. Peeters, N.J. Mason, P.J. Walker. Phys. Rev. Lett. **79**, *16*, 3034 (1997).
[11] Y. Naveh, B. Laikhtman. Appl. Phys. Lett. **66**, *15*, 1980 (1995).
[12] I. Knez, R.R. Du, G. Sullivan. Phys. Rev. B **81**, *20*, 201301(R) (2010).
[13] H. Kroemer. Physica E **20**, 196 (2004).
[14] A. Zakharova, S.T. Yen, K.A. Chao. Phys. Rev. B **64**, *23*, 235332 (2001).
[15] A. Zakharova, S.T. Yen, K.A. Chao. Phys. Rev. B **66**, *8*, 085312 (2002).
[16] F. Nichele, A.N. Pal, P. Pietsch, T. Ihn, K. Ensslin, C. Charpentier, W. Wegscheider. Phys. Rev. Lett. **112**, *3*, 036802 (2014).
[17] X. Shi, W. Yu, Z. Jiang, B.A. Bernevig, W. Pan, S.D. Hawkins, J.F. Klem. J. Appl. Phys. **118**, *13*, 133905 (2015).
[18] I. Knez, C.T. Rettner, S.-H. Yang, S.S.P. Parkin, L. Du, R.-R. Du, G. Sullivan. Phys. Rev. Lett. **112**, *2*, 026602 (2014).
[19] A. Hospodková, E. Hulicius, J. Pangrác, F. Dominec, M.P. Mikhailova, A.I. Veinger, I.V. Kochman. J. Cryst. Growth **464**, 206 (2017).
[20] M.P. Mikhailova, E.V. Ivanov, L.V. Danilov, K.V. Kalinina, N.D. Stoyanov, G.G. Zegrya, Yu.P. Yakovlev, E. Hulicius, A. Hospodková, J. Pangrác, M. Zíkova. J. Appl. Phys. **112**, *2*, 023108 (2012).
[21] M.P. Mikhailova, A.N. Titkov. Semicond. Sci. Technol. **9**, *7*, 1279 (1994).
[22] M.P. Mikhailova, K.D. Moiseev, Yu.P. Yakovlev. Semicond. Sci. Technol. **19**, *10*, R109 (2004).
[23] R.V. Parfeniev, K.D. Moiseev, V.A. Berezovets, N.S. Averkiev, M.P. Mikhailova, V.I. Nizhankovskii, D. Kaczorowski. J. Magn. Magn. Mater. **321**, *7*, 712 (2009).
[24] N.S. Averkiev, V.A. Berezovetz, M.P. Mikhailova, K.D. Moiseev, V.I. Nizhankovkiy, R.V. Parfiniev, K.S. Romanov. FTT **46**, *11*, 2083 (2004). (in Russian).
[25] Z. Wilamowski, A. Wolos, H. Rzybylinska. Curr. Top. Biophys. **33**, 257 (2010).
[26] A.I. Veinger, A.G. Zabrodskii, T.V. Tisnek, S.I. Goloshchapov, P.V. Semenikhin. ZhTF **83**, *12*, 103 (2013). (in Russian).
[27] Dzh. Ludvig, G. Vudberi. Elektronnyi spinovyi rezonans v poluprovodnikakh. Mir, M. (1964). 148 p. (in Russian).
[28] A.I. Veinger, A.G. Zabrodskii, T.L. Makarova, T.V. Tisnek, S.I. Goloshchapov, P.V. Semenikhin. ZhETF **143**, *5*, 918 (2013) (in Russian).
[29] A. Zabrodskii, A. Veinger, P. Semenikhin. Phys. Status Solidi B **257**, *1*, 1900249 (2020).
[30] H. Linke, P. Omling, P. Ramvall, B.K. Meyer, M. Drechsler, C. Wetzel, R. Rudeloff, F. Scholz. J. Appl. Phys. **73**, *11*, 7533 (1993).
[31] A.I. Veinger, A.G. Zabrodskii, T.V. Tisnek, G. Biskupski. FTP **32**, *5*, 557 (1998). (in Russian).
[32] A.I. Veinger, A.G. Zabrodskii, T.V. Tisnek. Phys. Status Solidi B **218**, *1*, 189 (2000).
[33] V.I. Veinger, A.G. Zabrodskii, T.V. Tisnek, S.I. Goloshchapov. Phys. Status Solidi C **5**, *3*, 835 (2008).
[34] A.I. Veinger, A.G. Zabrodskii, T.V. Tisnek, S.I. Goloshchapov. FTP **45**, *10*, 1314 (2011). (in Russian).
[35] P. Omling, B. Meyer, P. Emanuelsson. Appl. Phys. Lett. **58**, *9*, 931 (1991).
[36] Ch. Pul. Tekhnika EPR-spektroskopii. Mir, M. (1970), 560 p. (in Russian).
[37] D. Shenberg. Magnitnye ostsillyatsii v metallakh. Mir, M. (1986), 680 p. (in Russian).
[38] H.J. von Bardeleben, Y.Q. Jia, M.O. Manasreh, C.E. Stuz. Appl. Phys. Lett. **62**, *1*, 90 (1993).
[39] D.G. Seiler, W.M. Becker, L.M. Roth. Phys. Rev. B **1**, *2*, 764 (1970).
[40] P. Weightman, D.S. Martin, R.J. Cole, T. Farrell. Rep. Prog. Phys. **68**, *6*, 1251 (2005).
[41] W. Richter, J.-T. Zettler. Appl. Surf. Science **100–101**, 465 (1996).
[42] K. Möller, L. Töben, Z. Kollonitsch, Ch. Giesen, M. Heuken, F. Willig, T. Hannappel. Appl. Surf. Sci. **242**, *3–4*, 392 (2005).
[43] O.J. Pitts, S.P. Watkins, C.X. Wang. J. Cryst. Growth **248**, 249 (2003).
[44] M.S. Daly, D. Symons, M. Lakrimi, R. Nicholas, N. Mason, P. Walker. Semicond. Sci. Technol. **11**, *5*, 823 (1996).
[45] D.G. Seiler, A.E. Stephens. In: Landau Level Spectroscopy, Modern Problems in Condensed Matter Sciences, V. 27.2 / Ed. G. Landwehr, E.I. Rashba. Elsevier, North-Holland (1991). P. 1031.
[46] M. Dobrowolska, Y. Chen, J.K. Furdyna, S. Rodriguez. Phys. Rev. Lett. **51**, *2*, 134 (1983).
[47] D. Kindl, J. Toušková, E. Hulicius, J. Pangrác, T. Šimeček, V. Jurka, P. Hubík, J.J. Mareš, J. Krištofik. J. Appl. Phys. **95**, *4*, 1811 (2004).
[48] I. Knez, R.-R. Du, G. Sullivan. Phys. Rev. Lett. **107**, *13*, 136603 (2011).

[49] M.P. Mikhailova, A.I. Veinger, I.V. Kochman, P.V. Semenikhin, K.V. Kalinina, R.V. Parfeniev, V.A. Berezovets, A. Hospodková, J. Pangrác, E. Hulicius. Proc. SPIE **9755**, 97552R (2016).
[50] M.P. Mikhailova, A.I. Veinger, I.V. Kochman, P.V. Semenikhin, K.V. Kalinina, R.V. Parfeniev, V.A. Berezovets, M.O. Safonchik, A. Hospodková, J. Pangrác, M. Zíkova, E. Hulicius. J. Nanophotonics **10**, *4*, 046013 (2016).
[51] S.A. Tarasenko. FTT **44**, *9*, 1690 (2002). (in Russian).
[52] V.A. Kul'bachinskii, L.N. Oveshnikov, R.A. Lunin, N.A. Yuzeeva, G.B. Galiev, E.A. Klimov, P.P. Mal'tsev. FTP **49**, *2*, 204 (2015). (in Russian).
[53] E.A. de Andrada e Silva. Phys. Rev. B **46**, *3*, 1921 (1992).
[54] N.S. Averkiev, L.E. Golub. Phys. Rev. B **60**, *23*, 15582 (1999).
[55] R. Winkler. Spin–orbit coupling effects in two-dimensional electron and hole systems. Springer-Verlag, Berlin-Heidelberg (2003). P. 69.
[56] G.E. Pikus, V.A. Marushchak, A.N. Titkov. FTP **22**, *2*, 185 (1988). (in Russian).
[57] M. Cardona, N.E. Christensen, G. Fasol. Phys. Rev. B **38**, *3*, 1806 (1988).
[58] Handbook Series on Semiconductor Parameters / Ed. M. Levinshtein, S. Rumyantsev, M. Shur. World Scientific, London (1996). V. 1. 232 p.
[59] I. Žutić, J. Fabian, S. Das Sarma. Rev. Mod. Phys. **76**, *2*, 323 (2004).
[60] V.E. Degtyarev, S.V. Khazanova, A.A. Konakov. FTP **51**, *11*, 1462 (2017). (in Russian).
[61] C.S. Knox, L.H. Li, M.C. Rosamond, E.H. Linfield, C.H. Marrows. Phys. Rev. B **98**, *15*, 155323 (2018).
[62] D.M. Symons, M. Lakrimi, M. van der Burgt, T.A. Vaughan, R.J. Nicholas, N.J. Mason, P.J. Walker. Phys. Rev. B **51**, *3*, 1729 (1995).
[63] E.E. Mendez, L. Esaki, W.I. Wang. Phys. Rev. B **33**, *4*, 2893 (1986).
[64] G. Bastard, E.E. Mendez, L.L. Chang, L. Esaki. Phys. Rev. B **26**, *4*, 1974 (1982).
[65] I.V. Kochman, M.P. Mikhailova, A.I. Veinger, RV. Parfen'ev. FTP **55**, *4*, 313 (2021). (in Russian).
[66] I.A. Dmitriev, A.D. Mirlin, D.G. Polyakov, M.A. Zudov. Rev. Mod. Phys. **84**, *4*, 1709 (2012).
[67] D.C. Tsui, Th. Englert, A.Y. Cho, A.C. Gossard. Phys. Rev. Lett. **44**, *5*, 341 (1980).
[68] P. Kumaravadivel, M.T. Greenaway, D. Perello, A. Berdyugin, J. Birkbeck, J. Wengraf, S. Liu, J.H. Edgar, A.K. Geim, L. Eaves, R.K. Kumar. Nature Commun. **10**, 3334 (2019).
[69] M.A. Zudov, I.V. Ponomarev, A.L. Efros, R.-R. Du, J.A. Simmons, J.L. Reno. Phys. Rev. Lett. **86**, *16*, 3614 (2001).
[70] A.T. Hatke, M.A. Zudov, L.N. Pfeiffer, K.W. West. Phys. Rev. Lett. **102**, *8*, 086808 (2009).
[71] Yu.A. Firsov, V.L. Gurevich, R.V. Parfen'ev, S.S. Shalyt. Phys. Rev. Lett. **12**, *24*, 660 (1964).
[72] M.P. Mikhailova, V.A. Berezovets, R.V. Parfen'ev, L.V. Danilov, M.O. Safonchik, A. Hospodkova, J. Pangrac, E. Hulicius. FTP **51**, *10*, 1393 (2017). (in Russian).

Translated by M.Shevelev